

**DEVELOPMENT OF SELF-GRAVITATIONAL ADAPTIVE MESH REFINEMENT FOR SIMULATING BINARY STAR FORMATION.** Tomoaki Matsumoto, *Department of Humanity and Environment, Hosei University, Fujimi, Chiyoda-ku, Tokyo, 102-8160, Japan, (matsu@i.hosei.ac.jp).*

**Introduction:** A self-gravitational adaptive mesh refinement (AMR) code is newly developed for simulating protostellar collapse and fragmentation of a cloud core.

It is widely accepted that binary and multiple stars form as a result of fragmentation in a collapsing molecular cloud core [1]. Fragmentation of a molecular cloud core has been investigated through numerical simulations by many authors in the last two decades.

In order to follow the protostellar collapse and fragmentation, extremely wide dynamic range of spatial resolution is required of a numerical scheme. An initial condition of protostellar collapse is a molecular cloud core, of which size is  $\sim 0.01 - 0.1$  pc. On the other hand, a fragment, a seed of a binary star, has a radius of only  $\sim 1$  AU. Wide spatial dynamic range of  $\sim 10^{3-4}$  is therefore required to resolve both the entire cloud core and the small fragments. Truelove et al. [2] indicates that sufficient resolution is necessary for avoiding artificial fragmentation during protostellar collapse calculations (the Jeans condition). The AMR is one of the most popular technique to obtain the resolution with wide dynamic range in the recent simulations [2,3,4,5].

In this paper, implementation of a new AMR code is presented, and preliminary results with the code is also shown.

**Implementation:** The AMR code is vectorized and parallelized on the supercomputer Fujitsu VPP5000. The MPI library is used for parallelization. The entire code is written in FORTRAN90. The AMR code consists of three parts: (1) grid generation, (2) hydrodynamics, and (3) self-gravity.

**Grid Generation:** Block-structured grids are adopted for grid configuration. Each block has  $N_x \times N_y \times N_z$  cubic cells, where  $N_x$ ,  $N_y$ , and  $N_z$  denote the number of cells in the  $x$ ,  $y$ , and  $z$  directions, and they are constant over the blocks. The results with  $N_x = N_y = N_z = 8$  are shown here. The number of cells within a block is fixed, but the cell width differs depending on the grid-level; the cell width of each grid-level decreases successively by a factor of 2. The coarsest grid-level is labeled  $\ell = 0$  (the base grid), and the  $\ell$ -th grid-level has  $2^\ell$  times higher spatial resolution than the coarsest grid-level.

Data is stored by octree structure; the parent (coarse) block is linked with eight fine (children) blocks. Moreover, a block is linked with its neighbor blocks.

As a cloud collapses, small structures form in the dense region. When a block capturing the dense region satisfies a criterion for grid generation, eight finer blocks are automatically generated from the parent block, obtaining finer resolution. In the present calculations, the criterion of  $\lambda_J/8 < h$  is employed, where  $\lambda_J$  and  $h$  denote the Jeans length and the cell width of the parent block. This criterion satisfies the Jeans condition introduced by Truelove et al. [2].

**Hydrodynamics:** The hydrodynamics method for the AMR has been developed by extending the method for a nested grid [6]. The solver is based on Roe method [7], but has

been extended for solving the ideal, barotropic equations of state. A MUSCL approach and predictor-corrector method are adopted here for integration over time in order to achieve second-order accuracy in space and time. A multi-timestep scheme is adopted, and all the numerical fluxes are conserved at the interfaces between the adjacent blocks, and even between coarse and fine blocks [8].

**Self-Gravity:** Self-gravity is updated in every time step across all grid-levels by using the multigrid iteration for the Poisson equation. The method shows fast convergence of the solution; a residual reduces by a factor  $\sim 10^{-3}$  by each iteration. The numerical flux of gravity, which is equivalent to the gravitational force, is also conserved at the interfaces between the adjacent blocks, similarly to the hydrodynamics method described above. This flux conservation means that a field line of gravity never ends at the interface, leading to accurate evaluation of gravitational torque [11].

The method consists of three parts: (1) a full multigrid (FMG) scheme on the AMR grid, (2) V-cycle full approximation scheme (FAS) on the AMR grid, and (3) FMG for the base grid. In the first FMG scheme, the solution is converged simultaneously over the fine and coarse grids (composite grids corresponding to the hierarchy of grids). The composite grids are coarsen during the FMG cycle, so that the number of cells per block decreases from  $N_x \times N_y \times N_z$  to  $2^3$ . The solution on these  $2^3$  cells is converged further by the V-cycle FAS, and the FMG for the base grid.

**Application to Binary Formation:** Using the present AMR code, fragmentation during protostellar collapse is followed for the same model as Matsumoto & Hanawa [6]. Figure 1 shows the initial condition by cross-section. At the initial stage, the cloud core has density distribution factor of 1.1 denser than that of the critical Bonner-Ebert sphere [9, 10], and rotates rigidly at angular velocity of  $\Omega = 0.1 t_{\text{ff}}^{-1}$ , where  $t_{\text{ff}}$  denotes the initial freefall timescale at the cloud center and defined as  $t_{\text{ff}} = (3\pi/32G\rho_c)^{1/2}$ . The cloud also includes a velocity perturbation of  $m = 3$  mode with a very small amplitude ( $10^{-3}$ ) to break the point symmetry. The initial central density is  $\rho_c = 1 \times 10^{-19}$  g cm $^{-3}$ , the temperature is  $T = 10$  K, the radius of the cloud core is  $R_c = 0.144$  pc, and the mass of the cloud is  $M_c = 3.24 M_\odot$ . The parameter  $\alpha (= E_{\text{th}}/|E_{\text{grav}}|)$  has been discussed in terms of instability against fragmentation, where  $E_{\text{th}}$  and  $E_{\text{grav}}$  are thermal energy and gravitational energy. The model cloud has  $\alpha = 0.765$ .

A barotropic equation of state is adopted:  $P = c_s^2 \rho$  for  $\rho < \rho_{\text{cr}}$ , and  $P = c_s^2 \rho_{\text{cr}} (\rho/\rho_{\text{cr}})^{7/5}$  for  $\rho \geq \rho_{\text{cr}}$ , where  $P$ ,  $c_s$ , and  $\rho_{\text{cr}}$  denote pressure, isothermal sound speed, and the critical density for switching the equation of state. We set  $c_s = 0.19$  km s $^{-1}$ , and  $\rho_{\text{cr}} = 2 \times 10^{-13}$  g cm $^{-3}$ .

The cloud core undergoes the isothermal runaway collapse in the early stage, and an adiabatic core forms at the cloud center after the maximum density exceeds the critical density  $\rho_{\text{cr}}$ .

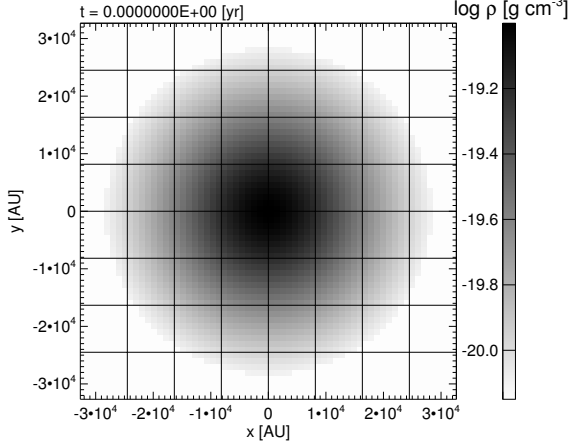


Figure 1: Density distribution in the mid-plane for the initial condition. The vertical and horizontal lines represent the block structure (boundaries of the blocks), and each block contains  $8^3$  cells. The cloud core is a factor 1.1 denser than the critical Bonner-Ebert sphere, and rotates at the angular velocity of  $\Omega = 0.1t_{\text{ff}}^{-1}$ .

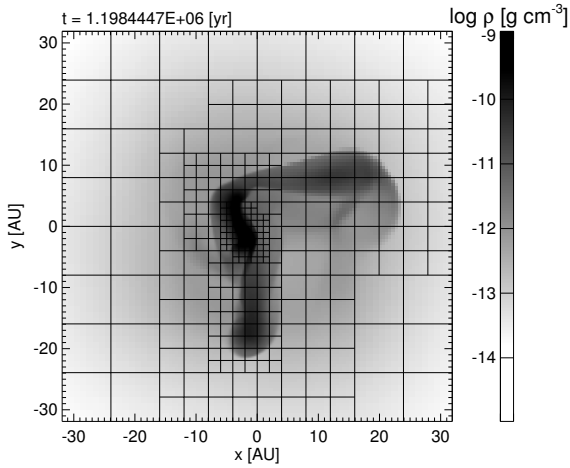


Figure 2: Same as Fig. 1 but for the stage of fragmentation. The oblate adiabatic core deforms to a ring-shape and then to a bar-shape. This figure shows grid-level of  $\ell = 10 - 13$ . Note that the spatial scale is different from Fig. 1 by magnifying by a factor of  $10^3$ .

The adiabatic core has an oblate shape; its radius and thickness are 6 AU and 3 AU, respectively. The oblate adiabatic core deforms to a ring shape temporarily, and then to a bar shape. The bar-shaped adiabatic core breaks into two fragments as shown in Figure 2. The fragments evolve to a proto-binary system 100 yr after the fragmentation, as shown in Figure 3. The binary system is surrounded by a circumbinary disk having spiral arms. One of the large spiral arms extending out in the  $y$ -direction evolves to an additional adiabatic core because of self-gravity. The new adiabatic core rotates around the central binary system, and the whole system becomes a hierarchical triple system as shown in Figure 4. The separation

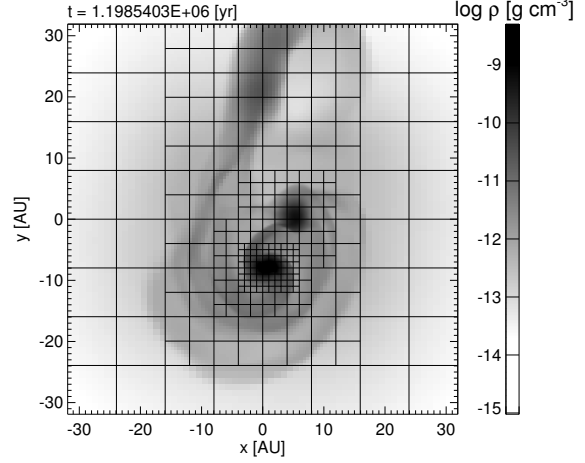


Figure 3: Same as Fig. 1 but for the stage of binary formation. This figure shows grid-level of  $\ell = 10 - 13$ .

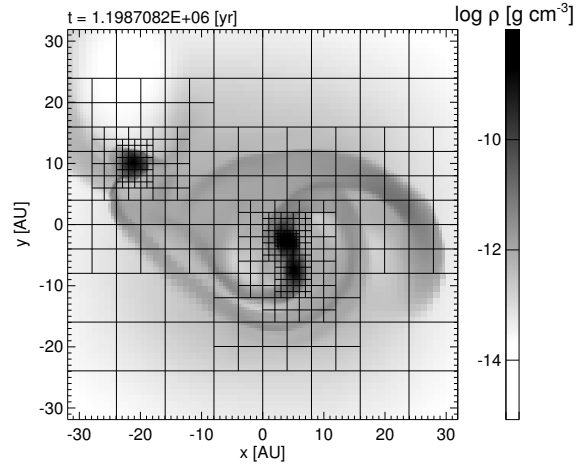


Figure 4: Same as Fig. 1 but for the stage of hierarchical triple system formation. This figure shows grid-level of  $\ell = 10 - 14$ .

between the central adiabatic cores is  $\sim 10$  AU, while the new adiabatic core is separated by  $\sim 30$  AU from the central close system. The orbits of the adiabatic cores seem to evolve in the further stages as indicated by Matsumoto & Hanawa [6]. The overall evolution is also consistent with that of Matsumoto & Hanawa [6].

**References:** [1] Bodenheimer, P., Burkert, A., Klein, R. I., & Boss, A. P. 2000, *Protostars and Planets IV*, 675. [2] Truelove, J. K. et al, 1997, *ApJ*, 489, L179. [3] Klein, R. I. et al. 2004, *ASP Conf. Ser.* 323, 227. [4] Banerjee, R., Pudritz, R. E., & Holmes, L. 2004, *MNRAS*, 355, 248. [5] Ziegler, U. 2005, *A&A*, 435, 385. [6] Matsumoto, T. & Hanawa, T. 2003a, *ApJ*, 583, 296. [7] Roe, P. L. 1981, *J. Comput. Phys.* 43, 357. [8] Chiang, Y., van Leer, B., & Powell, K. G. 1992, *AIAA 92-0443*. [9] Bonnor, W. B. 1956, *MNRAS*, 116, 351. [10] Ebert, R. 1955, *Z. Astrophys.*, 37, 222. [11] Matsumoto, T. & Hanawa, T. 2003b, *ApJ*, 595, 913.